Key Engineering Materials
ISSN: 1662-9795, Vol. 1056, pp 27-32
doi:10.4028/p-zW5TBc
© 2026 The Author(s). Published by Trans Tech Publications Ltd, Switzerland.
Submitted: 2025-09-13
Revised: 2025-12-20
Accepted: 2026-02-23
Online: 2026-05-20

4H-SiC Tunneling Light Emitter as a Light-Source for Quantum Applications

Jan Frederik Dick[1,a*], Samuel Ultsch[1,b], Mathias Rommel[2,c] and Jörg Schulze[1,2,d]

[1]Friedrich-Alexander-Universität Erlangen-Nürnberg, Chair of Electron Devices, Cauerstraße 6, 91058 Erlangen, Germany

[2]Fraunhofer Institute for Integrated Systems and Device Technology IISB, Schottkystraße 10, 91058 Erlangen, Germany

[a*]jan.dick@fau.de, [b]samuel.ultsch@fau.de, [c]mathias.rommel@iisb.fraunhofer.de, [d]joerg.schulze@fau.de

Keywords: light emitter, quantum tunneling, tunneling enhanced emission, light-source, off-resonant excitation, silicon vacancy.

Abstract. We report a light emitter based on a 4H-SiC lateral Zener diode that is operated under reverse bias in the quantum tunneling regime. Wide bandwidth white light emission with a peak wavelength of 492 nm corresponding to the transition between the nitrogen donor state and the aluminum acceptor state and a full width half maximum breadth of 303 nm at room temperature is shown. The peak breadth can be attributed to the relative shift of the acceptor and donor levels in the high electric field within the space charge region under reverse bias. At the wavelength of 730 nm, which is commonly used for off-resonant excitation of silicon vacancy defects, the emitter achieves 43.1% of its peak intensity. The emitter shows no blue light peak corresponding to the transition between the donor level of nitrogen and the valence band at 391 nm, such as the LED spectrum under forward bias of the same diode does.

Introduction

Recent advances in color-center technology show promising results towards room-temperature sensor applications using the silicon vacancy in 4H-SiC (V_{Si}) [1]. For widespread use of this technology, it would be favorable to monolithically integrate all components for initialization and read-out of the V_{Si}. 4H-SiC offers the possibility of a complete CMOS process integration [2], as well as the integration of wave guides and other optical components for light transmission [3]. This is instrumental for the direct optical read-out [4] and the monolithic integration of V_{Si} in a sensor chip. Furthermore, for the true monolithic integration of such sensors, an integrated light source is needed for the excitation of the V_{Si}, which poses challenges due to the wide and indirect bandgap of 4H-SiC [5]. For this purpose, we propose a lateral 4H-SiC tunneling diode as light emitter for V_{Si} excitation, which shows white light in Zener breakdown containing the wavelength necessary for off-resonant excitation at 730 nm [6, 7], which is fabricated using a subset of a 4H-SiC CMOS process.

Experimental

Device Geometry and Fabrication.

The devices discussed here are lateral 4H-SiC Zener tunneling diodes, which were fabricated using a subset of steps of the 2 µm 4H-SiC CMOS process at Fraunhofer IISB described in Fig. 1 [2]. A schematic cross-section of the diodes structure is shown in Fig. 1. The diode features n- and p-type doped regions, each with a doping concentration of $5 \cdot 10^{19}$ cm^{-3} that overlap 2 µm to form the tunneling junction, which are implanted into a 10^{16} cm^{-3} n-type doped epitaxial 4H-SiC layer. The dopant species are aluminum for the p^+-region and nitrogen for the n^+-region, respectively. Passivation of the devices is provided through 400 nm of SiO_2 deposited using plasma enhanced chemical vapor deposition (PECVD). Contact windows are etched using buffered hydrofluoric acid.

This article is an open access article under the terms and conditions of the Creative Commons Attribution (CC BY) license (https://creativecommons.org/licenses/by/4.0)

The highly doped regions are thereafter contacted with nickel silicide contacts, which are formed by nickel aluminum alloy lift-off and subsequent rapid thermal annealing (RTA). Aluminum is sputtered and patterned using a dry etching process to contact the device.

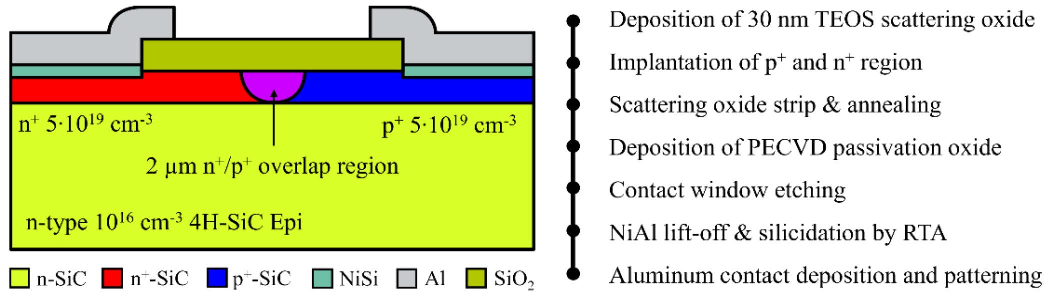

Fig. 1. Schematic cross-section of the lateral 4H-SiC Zener diode with overlapping n+ and p+ region and the corresponding fabrication process.

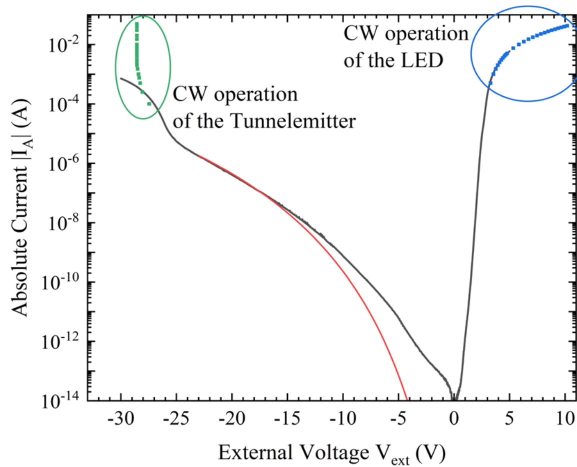

Fig. 2. Quasi-static current-voltage characteristic of the 4H-SiC Zener diode with the tunneling model by Kane [8] for reference in red under reverse bias. Additionally, the operation points of the diode for CW electroluminescence are shown for the LED operation in blue and in the tunnel emission regime in green.

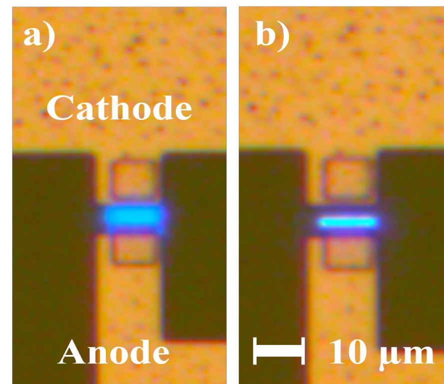

Fig. 3. Micrograph of the 4H-SiC Zener diode in operation under forward bias a) and under reverse bias b). The images were taken under the same ambient lighting conditions.

Optical and Electrical Characteristics.

The quasistatic electrical characteristic of the Zener diode is given in Fig 2. Under reverse bias a Zener tunneling current is observed, which can be approximated by the theory of tunneling by Kane [8] shown in red in Fig. 2. For the electroluminescent characterization, the diodes were operated at different positive and negative constant current biases in continuous wave (CW) operation. Under forward bias, at injection currents between 1 mA and 85 mA, marked in blue in Fig. 2, the diode emits a spectrum with two distinct peaks. Fig. 3 a) shows a micrograph of the emission under forward bias. The peak at 391 nm is attributed to the transition between the nitrogen donor state and the valence band, since the diode is in strong injection in this operation point and therefore free holes are available in the valence band for recombination. A second peak at 470 nm is visible, which is attributed to the transition between the nitrogen donor level and deeper defect levels in the bandgap as shown in Fig. 3 a) and in Fig. 4. This emission is known from literature [9, 10]. It is observed that the peak attributed to the donor-valence band transition grows faster with larger injection current than the peak of the donor-deep-level transition, which is shown in the inset of Fig. 4. Under reverse bias, light emission is observed at voltages beyond -27.4 V. Those operation points are marked in green in Fig. 2. It is visible that the quasistatic characteristic (shown in black) deviates from the operation points, in which

the diode was operated to acquire the CW spectra. This is due to self-heating of the device. At current biases above 4 mA the voltage drop across the device is constant for each injection current due to excessive self-heating of the device. Under the reverse current biases, the diode emits white light as shown in Fig 3 b) and Fig 5. The spectrum in Fig. 5 shows only one peak at 492 nm with a full width half maximum (FWHM) breadth of 303 nm. At 730 nm, which is commonly used as off-resonant excitation of V_{Si}, 43.1% intensity relative to the peak value remains, which makes this mode of emission viable for off-resonant excitation of V_{Si}. To avoid two color processes [11], or resonant excitation from the longer wavelength tail, passive optical band-pass filters, such as Bragg gratings [12] or plasmonic filters [13] must be co-integrated in future work for use in off-resonant excitation of V_{Si}. In the same way, the shorter wavelength peak must be suppressed to avoid excitation into the conduction band.

At low injection currents, the peak intensity of the tunnel emission scales linearly with the injected current up to 4 mA, where self-heating of the device results in constant bias across the junction at any applied current. This is shown in Fig. 6. With no further voltage drop across the junction, the peak intensity saturates. Furthermore, the linear relationship between the peak intensity and injection current in the current limited regime passes through the origin. Therefore, there is no threshold current density for tunneling enhanced light emission.

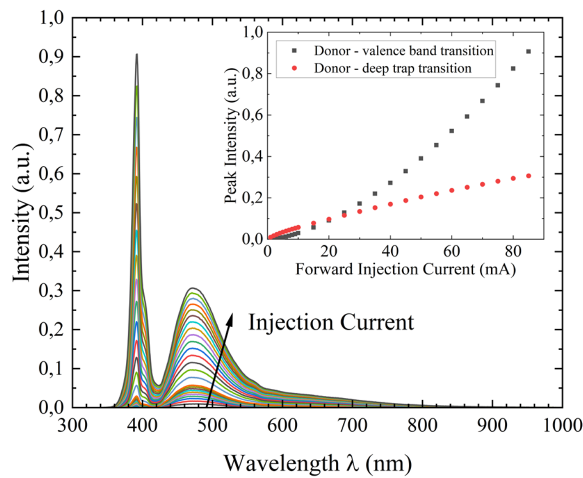

Fig. 4. Electroluminescence of the 4H-SiC Zener diode under forward current biases from 1 mA to 10 mA in 1 mA steps and from 10 mA to 85 mA in 5 mA steps. The inset shows the peak intensities of the two observed peaks with respect to the injection current.

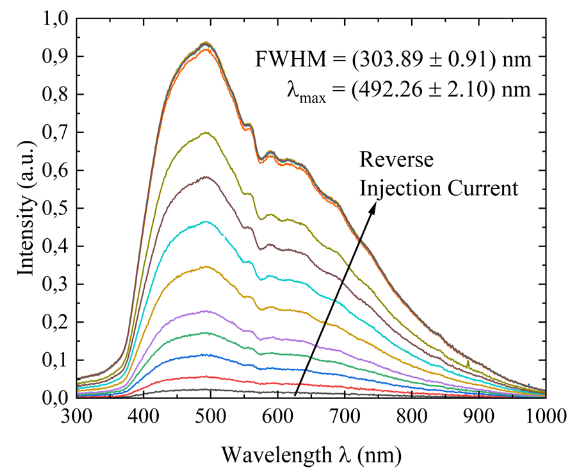

Fig. 5. Electroluminescence of the 4H-SiC Zener diode under reverse current biases from 100 µA to 50 mA. Above 4 mA of injection current the spectrum saturates, since the voltage drop across the diode stays the same due to self-heating.

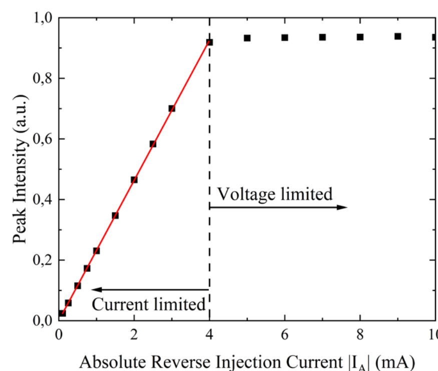

Fig. 6. Maximum intensity of the tunneling emission peak from Fig. 5 with respect to the injected current. Up to the point, where self-heating makes the voltage constant, the peak intensity is linear with respect to the injection current. Without change in voltage the spectrum saturates.

Discussion

The tunneling enhanced light emission is localized to the region exactly at the tunneling junction, which is shown in Fig 3 b). Therefore, it is assumed that the emission is localized to the high electric field region within the p-n junction. Consequently, a negligible amount of free charge carriers must be in the valence or the conduction band within the region of high electric field. This assumption is confirmed by the absence of a peak at 391 nm corresponding to a donor valence band transition. Free carriers that are generated through tunneling processes are quickly expelled from the space charge region. Within the region of high electric field, tunneling can happen from the valence band into any unoccupied defect within the bandgap, such as the nitrogen donor state. Since there are no holes available for optical transitions into the valence band, the only possible optical transitions are the ones between the nitrogen level and other trap states. At the p-n-junction, the p- and n-regions overlap, which makes the aluminum acceptor state the most available state that supports optical transition. The transition happens only when the acceptor state is unoccupied. This cascade of transitions is illustrated in Fig. 7 b). Since the acceptor state close to the valence band edge cannot be at the same position as the nitrogen donor, from which the electron recombines, an additional tunneling process during recombination is necessary. If the position of the acceptor state close to the valence band edge is shifted along the direction of the electric field, it also has a different energy level with respect to the donor state. Therefore, the energy of the emitted photon depends heavily on the distance r between the acceptor state and the donor state, the density of the acceptor states, the electric field strength, and the direction in which the defect is located.
The resulting spectrum from such a transition can be modeled by calculating the sum over all probabilities of tunneling from the donor state into an unoccupied acceptor state at a certain distance r with the photon energy E_{ph}. There are two probability components to this problem: First, the probability p_a of finding at least one acceptor state at distance r in the vicinity of the donor state. This expression is a function of the acceptor doping density N_A and formulated as the inverse problem of finding no acceptor state at distance r.

$$p_a = 1 - \exp\left(-N_A \frac{4}{3}\pi r^3\right) \tag{1}$$

Second, the tunneling probability p_t between the donor and the acceptor is necessary for the calculation. It is a function of the effective tunneling mass m^* and the tunneling barrier height E_b. The tunneling probability p_t can be given as:

$$p_t = \exp\left(-2\frac{\sqrt{2m^* E_b}}{\hbar} r\right) \tag{2}$$

To model the spectrum with respect to the photon energy E_{ph}, the probabilities of an electron recombining and tunneling from the donor into an acceptor state must be integrated over all radii r. The integration is possible since for each fixed distance r_0 around the donor, the energy of the acceptor states at that distance are uniformly distributed on the spherical shell with distance r_0 around the donor state. To arrive at an expression that is proportional to the intensity I_0 with respect to the photon energy E_{ph}, a relation between r_0 and E_{ph} is necessary. It is given by (3) and depends on the electric field $\mathcal{E}$:

$$r_0 = \frac{E_{ph} - E_b}{q\mathcal{E}} \tag{3}$$

Since the dependence of the intensity I_0 on the photon energy E_{ph} is of interest and each photon energy is correlated to a value of r_0, from which on it is part of the spherical shell, the integration must have a lower boundary of r_0 (correlated to E_{ph} in (3)) and a upper boundary of infinity. The expression can be written as follows:

$$I_0 \sim \int_{r_0}^{\infty} p_a(r)\, p_t(r)\, dr \tag{4}$$

The integral is not analytically solvable and is therefore numerically evaluated. For the numeric evaluation a fixed upper boundary of 50 nm is chosen, since the tunneling probability for this distance is negligible. Unknown parameters, such as the electric field inside the p-n junction and the effective tunneling mass between the states are used as fit parameters to approximate the spectrum from Fig. 5. Known parameters, such as the acceptor concentration N_A are fixed at the known value. In Fig. 8, the modeled spectrum is shown in red and the measured spectrum is shown in black. The parameters for the shown spectrum are a constant electric field of $5 \cdot 10^6$ V/cm, an effective tunneling mass of $0.018 \cdot m_0$, with m_0 being the electron mass in vacuum, the fixed acceptor density of $5 \cdot 10^{19}$ cm^{-3}, and a tunneling barrier height of 2.45 eV between the nitrogen donor and the aluminum acceptor. The model does correspond well to the measurement shown in Fig. 8 with respect to the breadth of the peak, its general shaping, and in terms of skew. The model still lacks the consideration of absorption around the bandgap energy of 4H-SiC, which explains the minimally steeper fall-off of the measured curve at the wavelength corresponding to the bandgap energy of 4H-SiC, as well as the consideration of band bending and inhomogeneous electric field at the recombination site, which explains the lower intensity of the measurement at large wavelengths. The deviation between 500 nm and 700 nm is attributed to reflections at the passivation oxide. The good accordance of the model and the measurement indicates that the proposed mechanism for the luminescence under strong reverse bias directly at the p-n junction is most likely a donor to acceptor transition, which is broadened by the variance of energy due to the relative position of donor and acceptor along the electric field.

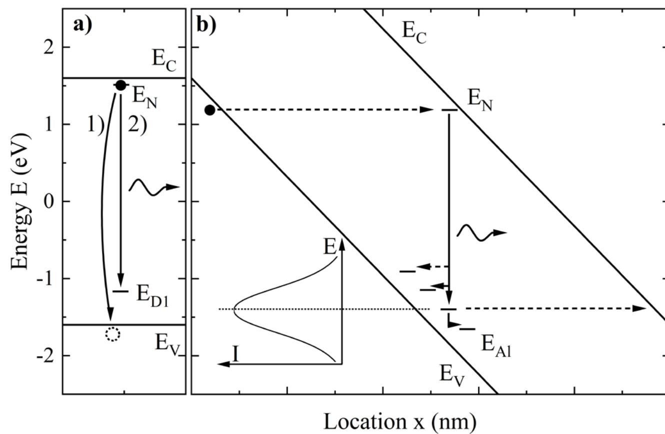

Fig. 7. Band diagram of the transitions observed under a) forward bias or b) the proposed mechanism for tunneling enhanced emission under reverse bias.

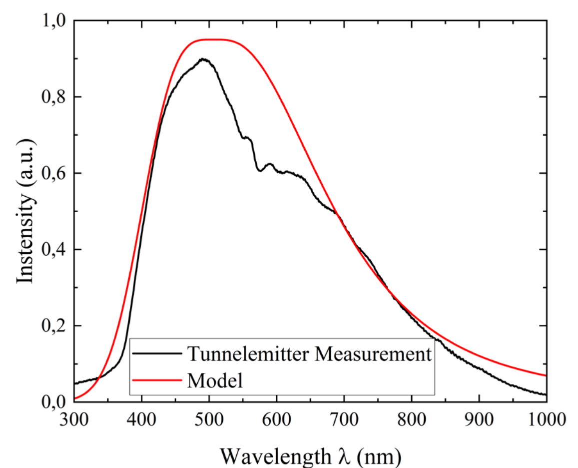

Fig. 8. Comparison between the measured spectrum of the tunneling light emitter and the proposed model with the empirically determined parameters for the effctive tunneling mass and the electric field.

Conclusion

In the tunneling enhanced light emission regime, optical transitions in 4H-SiC Zener diodes happen between states within the bandgap. Here, we dominantly observe the transition between the nitrogen donor state and the aluminum acceptor state. Due to the strong band bending, the states available for recombination have an energy distribution along the electric field, which leads to a broad spectrum below the bandgap energy of 4H-SiC. In this spectrum, the spectral component for the excitation of V_{Si} at 730 nm is contained with a relative intensity of 43.1% of the peak intensity. Further filtering of the spectrum for such excitation using passive optical filters is necessary and subject of future work.

Acknowledgment

We gratefully acknowledge the help of L. Baier with the measurement setup and the continuous support of the cleanroom staff at Fraunhofer IISB and LEB with the fabrication of the samples.

References

[1] S. Castelletto, C. T.-K. Lew, W.-X. Lin, and J.-S. Xu, "Quantum systems in silicon carbide for sensing applications," *Reports on progress in physics. Physical Society (Great Britain)*, vol. 87, no. 1, p. 14501, 2023.

[2] A. May, M. Rommel, L. Baier, M. Schraml, J.F. Dick, M.P.M. Jank, and J. Schulze, "A 4H-SiC CMOS technology enabling smart sensor integration and circuit operation above 500 °C," *2024 Smart Systems Integration Conference and Exhibition (SSI),Hamburg, Germany*, 2024.

[3] C. Babin *et al.,* "Fabrication and nanophotonic waveguide integration of silicon carbide colour centres with preserved spin-optical coherence," *Nat. Mater.*, vol. 21, no. 1, pp. 67–73, 2022.

[4] J. H. Schwarberg, R. Karhu, B. Kallinger, M. Rommel, R. Schmidt, and J. Schulze, "Investigation of CMOS Single Process Steps on 4H-SiC a-Plane Wafers for Quantum Applications," in *2024 47th MIPRO ICT and Electronics Convention (MIPRO)*, Opatija, Croatia, May. 2024 - May. 2024, pp. 1566–1572.

[5] M. E. Levinštejn, Ed., *Properties of advanced semiconductor materials GaN, AlN, InN, BN, SiC, SiGe*. New York, Weinheim: Wiley, 2001.

[6] M. Widmann *et al.,* "Electrical Charge State Manipulation of Single Silicon Vacancies in a Silicon Carbide Quantum Optoelectronic Device," *Nano Letters*, vol. 19, no. 10, pp. 7173–7180, 2019.

[7] R. Nagy *et al.,* "High-fidelity spin and optical control of single silicon-vacancy centres in silicon carbide," *Nat Commun*, vol. 10, no. 1, p. 1954, 2019.

[8] E. O. Kane, "Theory of Tunneling," *J. Appl. Phys.*, vol. 32, no. 1, pp. 83–91, 1961.

[9] H. Ou *et al.,* "Advances in wide bandgap SiC for optoelectronics," (in En;en), *Eur. Phys. J. B*, vol. 87, no. 3, pp. 1–16, 2014.

[10] A. Kar, K. Kundu, H. Chattopadhyay, and R. Banerjee, "White light emission of wide-bandgap silicon carbide: A review," *J Am Ceram Soc*, vol. 105, no. 5, pp. 3100–3115, 2022.

[11] T. Steidl *et al.,* "Single V2 defect in 4H silicon carbide Schottky diode at low temperature," *Nat Commun*, vol. 16, no. 1, p. 4669, 2025.

[12] J. H. Song *et al.,* "Grating devices on a silicon nitride technology platform for visible light applications," *OSA Continuum*, vol. 2, no. 4, p. 1155, 2019.

[13] S. Javid, F. T. Hamedani, P. Rezaei, and S. Khani, "Designing scalable single-mode to seven-mode plasmonic filters utilizing disk and ring-shaped resonators," *Results in Optics*, vol. 21, p. 100919, 2025.